

E. S. Lee · S. Y. Baek · C. R. Cho

A study of the characteristics for electrochemical micromachining with ultrashort voltage pulses

Received: 26 October 2004 / Accepted: 14 July 2005 / Published online: 20 December 2005
© Springer-Verlag London Limited 2005

Abstract Electrochemical micromachining (EMM) has traditionally been used in highly specialized fields, such as those of the aerospace and defense industries. It is now increasingly being applied in other industries, where parts with difficult-to-cut material, complex geometry and tribology, and devices of microscopic-scale are required. EMM, which is not normally considered as a precision process, is presented in this paper. The application of voltage pulses between a tool electrode and a workpiece in an electrochemical environment allows the three-dimensional machining of conducting materials with micrometer precision. In this paper, tool electrodes (5 µm in diameter, 1 mm in length) are developed by EMM and microholes are manufactured using these tool electrodes. Microholes with a size of below 50 µm in diameter can be accurately achieved by using ultrashort voltage pulses (1–5 µs).

Keywords Ultrashort voltage pulse · Electrochemical micromachining · Current efficiency · Double layer · Current density · Duty factor

1 Introduction

Recently, high-durable goods that are better than previous incarnations have been used to increase the durability of machine parts according to the development of industries.

Conventional mechanical machining is difficult to apply to machine parts that need to consider functional characteristics before mechanical or structural characteristics. There-

fore, non-conventional micromachining technology that is different from conventional machining needs to be applied to manufacture machine parts of a microshape effectively.

Micromachining techniques include: lithography, which is used in semiconductor processes; electro discharge machining (EDM); ultrasonic machining; and electrochemical machining, to name but a few. So, the electrochemical micromachining (EMM) technique, which is used to manufacture parts and is usually applied to semiconductor industries, is becoming less conspicuous.

EMM has seen a resurgence of industrial interest within the last decade, due to its many advantages, such as no tool wear, stress-free and smooth surfaces, and the ability to machine complex shapes in materials, regardless of their hardness and high strength, high tension, or whether they are heat-resistant materials. EMM can machine difficult-to-cut materials and complex shapes without distortion, scratches, burrs, or stress. It provides an effective alternative for manufacturing a wide range of components, such as aircraft turbine parts, surgical implants, bearing cages, molds and dies, and even microcomponents [1–3].

Electrical characteristics play a principal functional role and chemical characteristics play an assistant functional role in EMM. Therefore, essential parameters in EMM can be described as current density, machining time, inter-electrode gap size, electrolyte, electrode shape, etc.

EMM has been processed using DC current in the early days, but recently, micro pulse electrochemical machining (PECM), which can continue past micro-inter-electrode gaps, increases the accuracy of the shape and makes a better surface roughness using pulse current than surface roughness using DC current has been researched.

EMM can manufacture micro-shape machining with high efficiency and increase the dimensional accuracy and processing quality result in current convergence, which creates electrochemical dissolution on the anode actively because it can supply electrolyte and pulse current stably and continue through micro-inter-electrode gap sizes [4–6].

Knowledge of the mechanism is essential to apply EMM to machining. EMM techniques have been used in manufacturing micropores and shafts for a semiconductor test

E. S. Lee (✉)
Department of Mechanical Engineering,
Inha University,
253, Yonghyun-Dong, Nam-Gu,
Incheon, 402-751, South Korea
e-mail: leees@inha.ac.kr

S. Y. Baek · C. R. Cho
Graduate School of Mechanical Engineering,
Inha University,
Incheon, 402-751, South Korea

device, AFM (atomic force microscope), STM (scanning tunneling microscope), etc. [7–9].

Therefore, diverse parameters of EMM have been defined and applied. EMM, one of the non-traditional machining techniques, can be used to achieve a desired workpiece surface by dissolving the metal workpiece with mechanical and electrochemical reactions. Generally, the EMM method can be applied in industry for cutting, deburring, drilling, and shaping the workpiece, and has been used in aircraft parts and turbine blades, and rocket engines, but recently, this machining method is usually used to manufacture several microgrooves on the microbearings in a rotor [10].

The surface roughness of the machined workpiece is also a very important parameter. An ultra-precision product's quality could be decided according to the surface roughness. The surface roughness is improved when a pulsed electric current is supplied. The higher the increase in pulse frequency in the same current efficiency conditions and also the higher current efficiency increase in different electrical conditions, the more the surface roughness is improved in EMM [11]. It has been researched how the machining efficiency is affected by electrolyte concentration [10, 12].

It is found that a better accuracy of shape can be obtained in EMM when the pulse-on time used is in the range $0.1 \mu\text{s} \sim 0.5 \mu\text{s}$ and the pulse-off time used is in the range $5 \mu\text{s} \sim 50 \mu\text{s}$ [13].

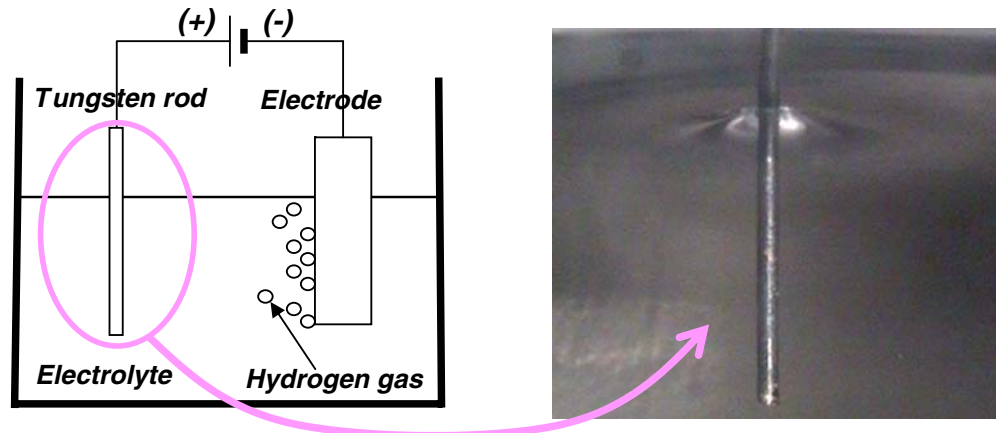
In this paper, the characteristics of EMM has been researched through simulations and experiments according to various parameters, such as voltages, currents, inter-electrode gap size, electrolyte concentrations, machining time, and duty factor. Also, the present studies were directed towards the identification and comparison of experimental results EMM according to a microprobe manufactured by electrochemical etching and then having EMM carried out for improving the dimensional accuracy.

2 Manufacturing of a microprobe

2.1 Principle of machining

When an electric current is passed between the electrode and a tungsten rod dipped into the electrolyte, a chemical

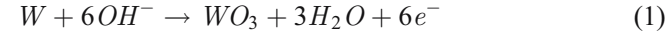
Fig. 1 Principle scheme of electrochemical etching



process occurs in the electrolyte tank. A typical example is that of the electrode and tungsten wires connected to a source of direct current and immersed in a solution of electrolyte, as shown in Fig. 1.

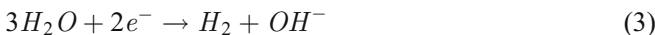
In typical manufacturing operations, as a potential difference is applied across the electrodes, several possible reactions can occur at the anode and cathode. With this metal–electrolyte combination, the electrolysis has caused the dissolution of iron from the anode, and the generation of hydrogen at the cathode. The oxidation reaction occurs at the anode because the metal lost an electron, which is changed into a metal ion dissolved in electrolyte, and the deoxidation reaction occurs at the cathode because the electrode obtains the ion, which is extracted to the atom or molecule. The technique for manufacturing the microprobe can be called electrochemical etching or the deep immersion method, and we obtained a microprobe by using those methods. The microprobe is manufactured first by utilizing an electrode, and then the tool size or shape are copied to the workpiece in EMM. Sources of electricity were applied across the cathode and anode with ultrashort pulse voltages.

A piece of tungsten carbide $100 \mu\text{m}$ in diameter was used as the workpiece and deoxidation platinum was used for the electrode. Sodium hydroxide electrolyte was used for processing the tungsten carbide. The tungsten carbide is dissolved at the anode with a chemical reaction by following equations:



Equation 1 denotes the process in which the atomic structure around the tungsten surface reacts with a hydroxide ion and Eq. 2 denotes the process in which the tungsten oxide which reacts again with a hydroxide ion, and is changed to an ion and dissolved with the electrolyte. The chemical reaction in the following equation occurs in the platinum electrode at the cathode. The platinum does

not react at all and the water molecule is divided into a hydrogen ion and an hydroxide ion:



Therefore, the reaction that hydrogen ions are changed to hydrogen gas occurs because they obtain electrons. The hydrogen gas generated formed a bubble and emerged from the surface of the cathode.

2.2 Machining of a microprobe

In this study, pre-machining was performed with a 4-V voltage for 20 s in sulfuric acid of 30% to remove the film of tungsten carbide on the surface. A tungsten carbide film on the workpiece often prevent the electrochemical reaction from occurring, but EMM could be performed after the film was removed.

High current density formed a diffusion layer surrounding the tungsten carbide as the dissolving velocity of metal is higher than the extracting velocity of metal ion. The thicker the diffusion layer, the lower the moving speed of the ions. Therefore, the dissolving speed of the metal is slowing down. The more tungsten carbide is dissolved, the greater the diffusion layer is increased. Otherwise, low current density can produce a sharp microprobe with a submicron-size probe tip as the oxide generation of the tip surface is slow. The condition for manufacturing a microprobe is shown in Table 1. Pulse voltages are applied and the interval of frequency and pulse were fixed. The microprobe was manufactured and compared according to the variable voltage.

2.3 Experimental results

The microprobes developed by electrochemical etching are shown in Figs. 2 and 3. Figure 2 shows the comparison between a microprobe machined by electrochemical etching and a hair. The manufactured microprobe was 10 μm or less in diameter. Examples of microelectrodes manufactured are shown in Fig. 3.

The tip of a microprobe with radius on the nanometer scale is shown in Fig. 3a. It can be achieved with low current density and voltage. Figure 3b shows the double-stepped microprobe. A high voltage of 4 V was applied and the shape of the reverse taper was obtained in first step and

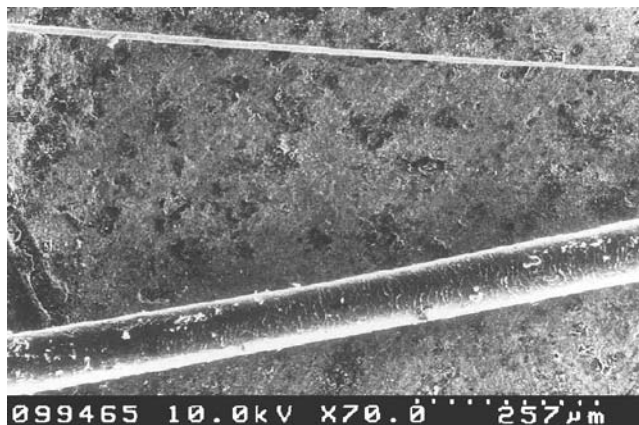


Fig. 2 Comparison of microprobe (10 μm) with hair (70 μm)

then the shape of the tip, which is sharp, was manufactured in the second step by applying a voltage of 0.8 V. The microprobe, which has a straightness of 1 mm in length was manufactured by applying a voltage of 1.5 V.

3 Electrochemical micromachining (EMM)

3.1 Principle and modeling of EMM

Electrochemical micromachining (EMM) is similar to electro-polishing in that it also is an electrochemical anodic dissolution process in which a direct current with high density and low voltage is passed between a workpiece and the cathode. At the anodic workpiece surface, metal is dissolved into metallic ions by the deplating reaction, and, thus, the tool shape is copied into the workpiece. The electrolyte is forced to supply through the inter-electrode gap with high velocity, usually more than 5 m/s, to intensify the mass-change transfer through the sub layer near the anode and to remove the sludge, heat, and gas bubbles generated in the gap.

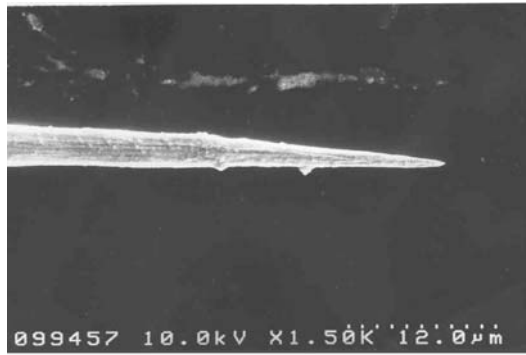
There are many factors which affect the machining property in EMM, especially, the current density and inter-electrode gap is very important. The fragmentary example is shown in Fig. 4.

The current density of the inter-electrode gap is higher than the one of the surrounding gaps, as the gap size of inter-electrode is so small. Therefore, the workpiece is machined firstly at the inter-electrode gap. If the inter-electrode gap size is lower, the current density distribution is unstable and then machining occurs as the load of the machining area is increased.

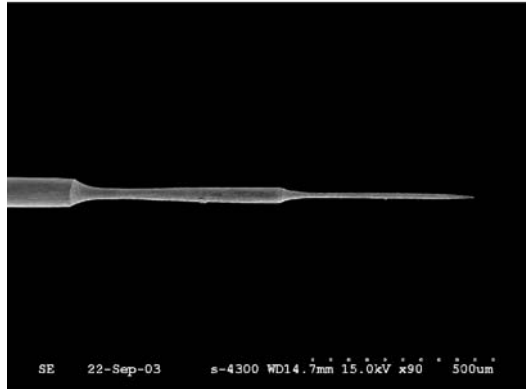
EMM with ultrashort pulse voltages could give rise to improvements in machining efficiency and accuracy. Electrolyte conductivity, acting as a resistance, has been recognized one of the most important parameters in EMM and is affected by heating and hydrogen gas generation. In this study, the parameter, combined electrolyte conductivity, is defined by the experimental results of the voltage-current value to contain both resistance of the mechanical system R_m and electrolyte R_e , as shown in Fig. 5.

Table 1 Experimental setup

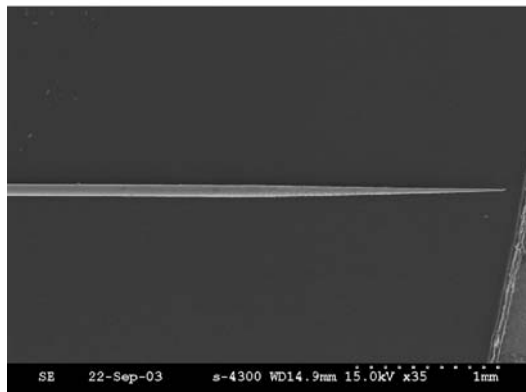
Voltage	0.8 V~4 V, variable pulse width
Frequency	1 kHz
Electrode tool (cathode)	Pt
Workpiece (anode)	Tungsten carbide rod
On/off duty	50%
Length	1 mm
Electrolyte	NaOH(2 M)



a Tip of micro probe



b Double stepped micro probe



c Straight micro probe

Fig. 3a–c Examples of microprobes. **a** Tip of a microprobe. **b** Double-stepped microprobe. **c** Straight microprobe

R_{e_small} is the electrolyte resistance of the shorter path between the tool and the workpiece, and R_{e_large} is that of the longer path. Because of the small gap, R_{e_small} is also small and, therefore, the machinable area is restricted to a localized region of the tool. When the voltage pulse with the on-time is applied between double layers, the electric current flows through the shorter path with the electrolyte resistance R_{e_small} and EMM occurs strongly in the localized area around the tool.

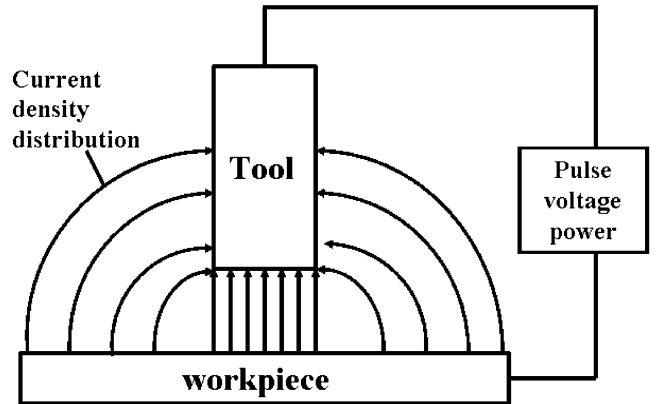


Fig. 4 Sketch of inhomogeneous current density distribution during EMM

The combined electrolyte conductivity κ_C can be expressed by Ohm's Law:

$$\kappa_C = \frac{Si}{E} \quad (4)$$

where S =gap size, i =current density, and E =voltage. The metal removal rate during the on-time can be obtained from Faraday's Law [14, 15]:

$$\frac{dS}{dt} = \frac{A\kappa_C(E_0 - \Delta E)}{Sz\rho_a F} - f \quad (5)$$

where E_0 =voltage pulse, ΔE =overpotential, and f =feed-rate of the electrode.

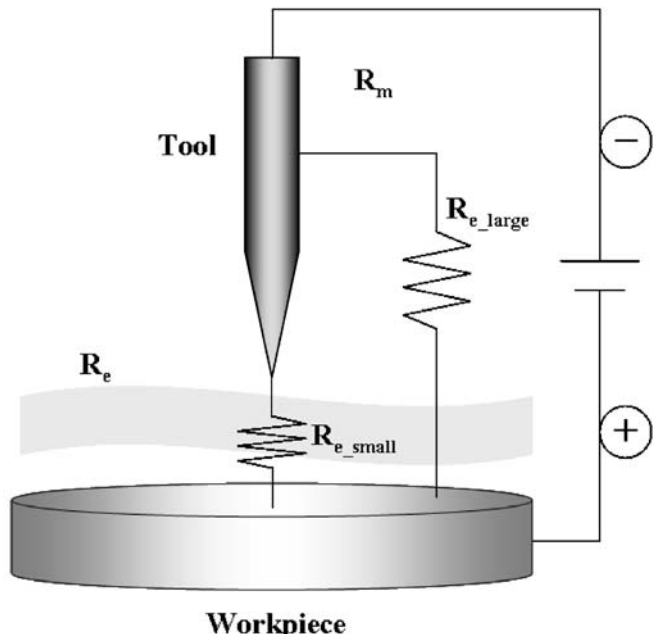


Fig. 5 Schematic diagram of an electrochemical cell. Combined electrochemical resistance contains both resistance of the mechanical system, R_m , and of the electrolyte, R_e

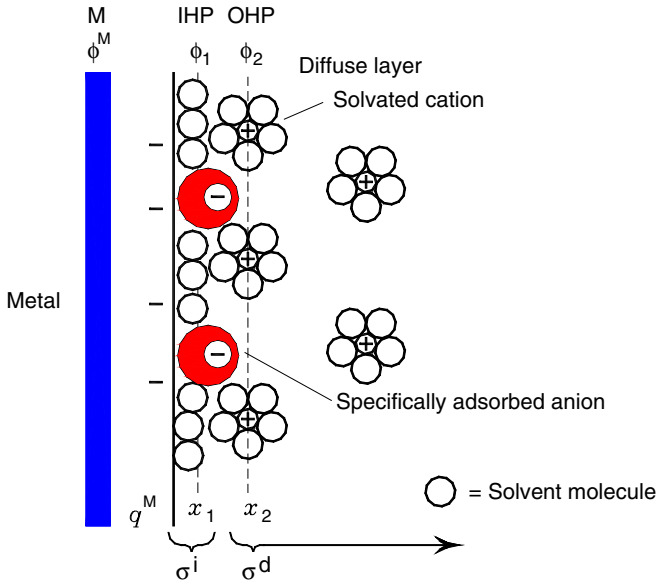


Fig. 6 The electrical double layer

There is no feed of electrode in the EMM of air-lubricated hydrodynamic grooves. The gap variation S from τ_{on} to τ_{off} can be expressed as:

$$\int_{\tau_{on}}^{\tau_{off}} S dS = \int_{\tau_{on}}^{\tau_{off}} \frac{A \kappa_C (E_0 - \Delta E)}{z \rho_a F} dt \quad (6)$$

By solving Eq. 5, the gap variation S is obtained as:

$$S_1 = \sqrt{S_0^2 + 2K_v \kappa_C Et} \quad (7)$$

$$K_v = \frac{A}{zF \rho_a}$$

where K_v , the effective volumetric electrochemical equivalent, is a constant defined by the anode workpiece.

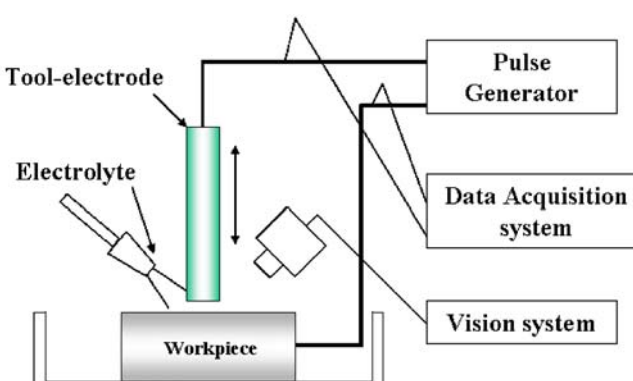


Fig. 7 Schematic diagram of electrochemical micromachining (EMM) process

Table 2 Typical experimental conditions in this study

Applied voltage	1.5 V~3 V, variable pulse width
Applied frequency	10 kHz~1 MHz
Electrode tool (cathode)	Tungsten carbide
Workpiece (anode)	STS 420 Disc
Pulse duration	100 ns~5 μ s
Electrolyte	HCl (0.5 M)

3.2 The electrical double layer

The solution side of the double layer is thought to be made up of several “layers.” The inner layer, which is closest to the electrode, contains solvent molecules and, sometimes, other species (ions or molecules) that are said to be specifically adsorbed in Fig. 6. This inner layer is also called the compact, Helmholtz, or Stern layer. The locus of the electrical centers of the specifically adsorbed ions is called the inner Helmholtz plane (IHP), which is at a distance x_1 . The total charge density from specifically adsorbed ions in this inner layer is σ^i (μ C/cm 2). Solvated ions can approach the metal only as far as a distance x_2 ; the locus of the centers of these nearest solvated ions is called the outer Helmholtz plane (OHP).

The interaction of the solvated ions with the charged metal involves only long-range electrostatic forces, so that their interaction is, essentially, independent of the chemical properties of the ions. These ions are said to be nonspecifically adsorbed. Because of thermal agitation in the solution, the nonspecifically adsorbed ions are distributed in a three-dimensional region called the diffuse layer, which extends from the OHP into the bulk of the solution.

3.3 Experimental device and method

The experimental device which can manufacture micro-holes and shapes using the microprobe developed earlier is

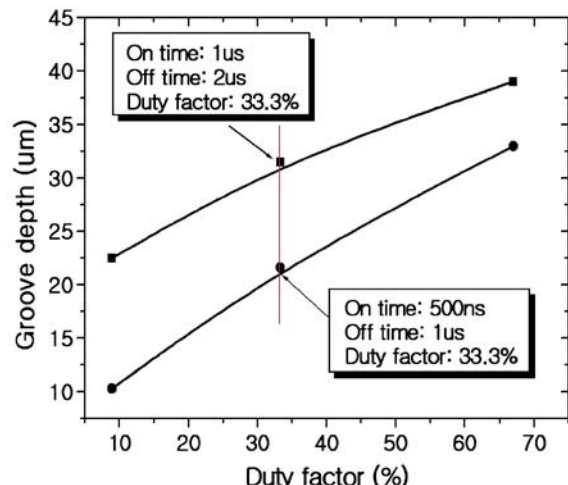
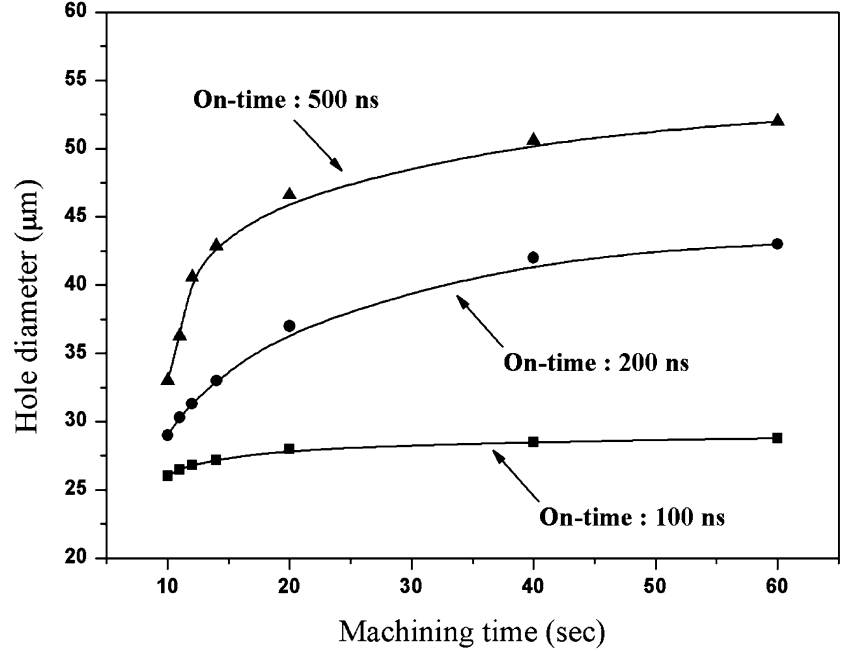


Fig. 8 A comparison of groove depth for the same duty factor but different pulse duration

Fig. 9 Hole diameter according to pulse-on time (1.5 V, 1- μ s pulse duration)

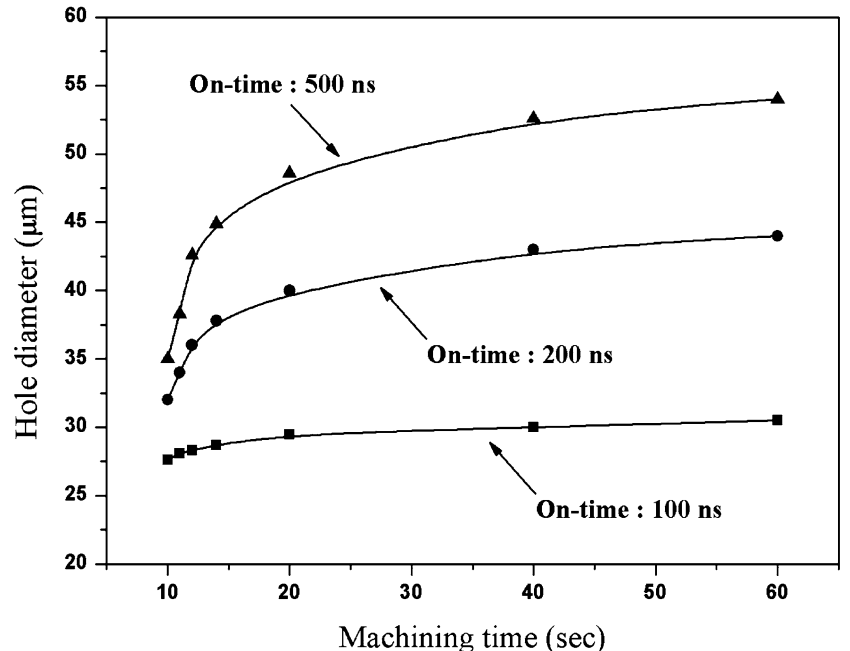


shown in Fig. 7. The experimental device used in this study has micro-feeding system with 12- μm resolution and the machining condition was checked by a microscope system in real time. This device consists of the system which can check signals generated when machining, a function generator which can make sources of electricity with pulse voltages, and a supply system of electrolyte which can generate the chemical reaction. The gap between the electrode and the workpiece was set to 100 μm using the

microfeeding system and the microscope system and 0.5 M of HCl electrolyte was supplied to the inter-electrode gap.

EMM is performed where the cathode and the anode chuck are connected to the negative terminal and positive terminal of power supply, respectively. Simultaneously, a three-dimensional structure was manufactured by means of controlling pulse and frequencies through the function generator. Typical experimental conditions in this study are shown in Table 2.

Fig. 10 Hole diameter according to pulse-on time (2 V, 1- μ s pulse duration)



4 Results and discussion

Generally, a duty factor is applied to classify each machining condition in the case of using a pulsed current, and is defined by following equation:

$$\text{Duty factor} = \frac{\tau_{on}}{\tau_{on} + \tau_{off}} \quad (8)$$

Figure 8 illustrates a comparison of groove depth for the same duty factor, but different pulse time. It is shown that the machining depth changes according to the duty factor. The duty factor has the same values of 33.3%, but the pulse on, off time is different. Namely, the machining depth is affected not by the duty factor, but by the pulse on, off time. Therefore, the material removal rate (MRR) is increased rapidly according to the pulse-on time in the EMM-applied pulse voltages. It is more efficient to control the pulse-off time for dimensional accuracy and high accuracy of shape and surface roughness in the workpiece can be obtained by using ultrashort pulse voltages.

In EMM, the hole size is determined by the tool size and the inter-electrode gap size. We manufactured the hole size variations according to the EMM conditions and machining time with a 20-μm tool.

The platinum balance electrode we used in this study was set for the compensation of the difference of voltage drops between the electrolyte and the two electrodes. Because of the relatively large immersed area of the workpiece compared with that of the tool, the resistance between the electrolyte and the workpiece is small and the voltage drop is also small. Microholes were machined for several times without tool feeding.

After machining, the hole diameter was measured at the top surface of the workpiece. These experiments were performed by changing the pulse-on time and the voltage between the tool and the workpiece with a pulse duration of 1 μs.

As shown in Figs. 9 and 10, the hole size increased as the pulse-on time and the applied voltage increase. With a 2-V and 500-ns pulse-on time, the hole diameter was about 58 μm after 60 s of machining. When 1.5 V is applied with the pulse-on time of 100 ns, the localized hole diameter is 27 μm after 10 s of machining. It should be noted from these graphs that the workpiece is dissolved rapidly at the initial stage of machining.

Figure 11 shows the variable hole shapes with different voltages. Microholes were machined according to different



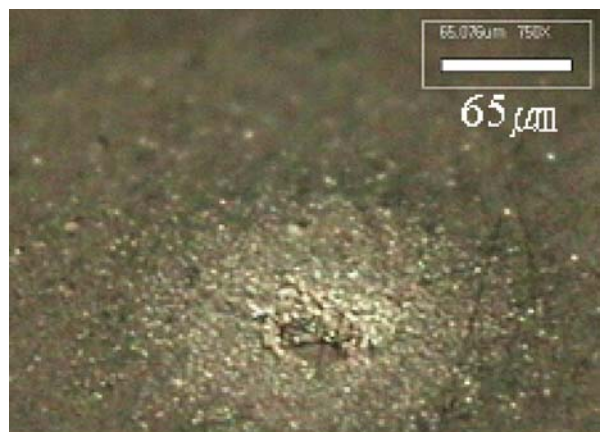
Fig. 11 Examples of hole shapes according to different voltages

machining conditions using the microprobe we already made.

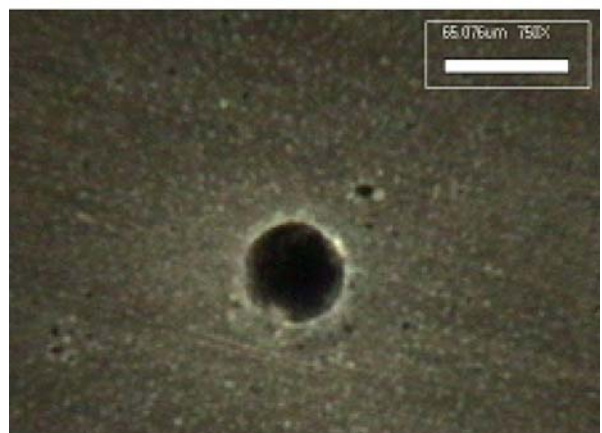
The more the voltages were increased, the greater the machining depths were increased in the same time, 1-μs pulse duration. Figure 12 shows that the machining accuracy of a microstructure was affected by the pulse interval in the same condition of voltages. The applied voltage and pulse duration time were 1.5 V and 5 μs, respectively, in Fig. 12a. The dispersion of current occurred at the inter-electrode gap and the accuracy of the shapes produced bad results due to that influence.

The applied voltage and pulse duration time were 1.5 V and 100 ns, respectively, in Fig. 12b. The diameter of the microprobe and microhole of the workpiece were 20 μm and 40 μm, respectively. Better shape accuracy of machining could be obtained from controlling the duration time of the pulse voltage.

Therefore, there was no more insulating material on the electrode to prevent the dispersion of current adjusting the ultrashort pulses and applying the pulse interval is very important in EMM.



a 5μs pulse duration (applied 1.5V)



b 100ns pulse duration (applied 1.5V)

Fig. 12a, b Photographs of microholes produced after different pulse duration times. **a** 5-μs pulse duration (applied voltage 1.5 V). **b** 100-ns pulse duration (applied voltage 1.5 V)

5 Conclusions

Electrochemical micromachining (EMM) using ultrashort pulses was studied in this paper. To remove the passive layer of tungsten carbide, the aqueous solution of H_2SO_4 (30%) served as the electrolyte. And various shapes and sizes of microprobes could be obtained using NaOH electrolyte and controlling the ultrashort pulse voltages in this study. The microprobe we developed in this study has a diameter of under 10 μm and the tip of the microprobe has a radius on the nanometer scale. And EMM was carried out using microprobe developed.

The aqueous solution of 0.5 M HCl was used and high-quality micro-holes with 40- μm diameter and 80- μm thickness stainless steel foil was machined. The future work, therefore, can be made when more engineering data has been gathered. In addition, more research needs to be done on related tests, such as surface roughness and shape accuracy using controlled ultrashort pulses controlled.

Acknowledgement This work was supported by the Inha University Research Foundation, Korea.

References

1. Datta M (1998) Applications of electrochemical microfabrication: an introduction. *IBM J Res Develop* 42(5):563–575
2. Rajurkar KP, Zhu D, Wei B (1998) Minimization of machining allowance in electrochemical machining. *Annals CIRP* 47(1): 165–168
3. McGeough JA (1974) Principles of electrochemical machining. Chapman Hall, London
4. Rajurkar KP, Zhu D, McGeough JA, Kozak J, De Silva A (2000) New developments in electrochemical machining. *Annals CIRP* 48(2):567–580
5. Schuster R, Kirchner VV, Allongue P, Ertl G (2000) Electrochemical micromachining. *Science* 289(5476):98–101
6. Wei B, Rajurkar KP, Talpallikar S (1997) Identification of interelectrode gap sizes in pulse electrochemical machining. *J Electrochem Soc* 144(11):3913–3918
7. In CH, Kim GM, Chu CN (2003) Fabrication of tungsten probe using electrochemical etching. *J KSPE* 18(2):111–118
8. Lim YM, Lim HJ, Kim SH (2001) Shape and diameter control of microshafts in electrochemical process. *J KSPE* 18(5):50–56
9. Zhu D, Xu HY (2002) Improvement of electrochemical machining accuracy by using dual pole tool. *J Mat Proc Tech* 129:15–18
10. Chikamori K (1998) Possibilities of electrochemical micro-machining. *Int J Jpn Soc Prec Eng* 32:37–38
11. Kim DH, Kang JH, Park KY (2000) Relationship between machining characteristics and current efficiency in electrochemical machining of Ni-Ti shape memory alloy. In: Proceedings of the KSMTE 2000 Fall Annual Meeting, pp 3–21
12. De Silva AKM, Altena HSJ, McGeough JA (2000) Precision ECM by process characteristic modelling. *Annals CIRP* 49(1): 151–155
13. Amalnik MS, McGeough JA (1996) Intelligent concurrent manufacturability evaluation of design for electrochemical machining. *J Mat Proc Tech* 61:130–139
14. Rajurkar KP, Wei B, Kozak J, McGeough JA (1996) Modeling and monitoring interelectrode gap in pulse electrochemical machining. *Annals CIRP* 44(1):177–180
15. Rajurkar KP, Wei B, Kozak J (1993) Study of pulse electrochemical machining characteristics. *Annals CIRP* 42(1):231–234